Design of an Optical Fibre-based Receiver System for Atmospheric Sensing Lidar

N. Sangeetha,*[1] Y. Bhavani Kumar,[2] and V.R. Machavaram [1]

[1]*School of Electronics Engineering, VIT University, Vellore-632014, India,*
[2]*National Atmospheric Research Laboratory, ISRO, Gadanki-517112, India*

Received July 13, 2015; accepted October 06, 2015; published December 31, 2015

Abstract—In this paper we report on the design of an optical fiber-based light receiver which is meant for replacing the conventional beam steering secondary mirror of the Newtonian telescope of a biaxial Raman lidar. The influence of using optical fibre, acting as an aperture stop of constant diameter on the geometrical compression form factor, as well as the transitional altitude and the resulting blur disk diameter have been determined. The viability of using a commercially available optical fibre as a receiver and the associated trade-offs have been discussed. A hot-fused fibre bundle-based receiver is proposed as a potential alternative for low altitude profiling to be enabled. These theoretical investigations have formed the basis for our current experimental work aimed at the development of all fibre-based reconfigurable beam delivery systems for mobile lidars.

Active remote sensing has been invoked for the past several decades. Technology evolution has simplified the design aspects and today's compact, regularized, novel configurations have been demonstrated [1]. For the past 40 years laser remote sensing of atmosphere has undergone tremendous technical changes. Areas like lasers, receivers and detectors have undergone sophisticated and miniaturized conceptual design. One among such areas is the fiber optic based light carrier technology [2].The application of fiber based design to a lidar has been attempted for the first time in India. This design uses the MM fiber in the UV spectral range. This design has been applied to an elastic Raman lidar used here.

The biaxial Raman lidar based in the National Atmospheric Research laboratory is mainly used for atmospheric water vapour profiling at night time. The Nd-YAG laser source operating at 532nm emits 100mJ/pulse at 10Hz repetition rate. A 10mm diameter beam exits the laser with a divergence of 0.5mrad. A Newtonian telescope with a parabolic primary mirror of 350 mm in diameter and focal length of 1000mm, in conjunction with a beam steering secondary plane mirror of 100mm in diameter is used for collecting the atmosphere backscattered light. The presence of a secondary mirror obscures the collection of back scattered light around the telescope axis. It was reported previously that an optical fibre-based receiver can reduce the obscuration loss due to its small size [3]. The following section presents the calculations leading to the choice of a suitable commercial fibre for backscattered light collection at the location of a secondary mirror.

* E-mail: nsangeetha@vit.ac.in

The backscattered light signal P(R) of a lidar can be expressed as [4]:

$$P(R)=KE(R)\beta(R)T(R), \tag{1}$$

where K is the system efficiency factor; $\beta(R)$ is the backscatter coefficient at an altitude R; $T(R)$ represents round trip losses due to absorption and scattering; and $E(R)$ is the geometrical compression form factor defined as:

$$E(R)=\xi(R)/R^2 , \tag{2}$$

where $\xi(R)$ is the overlap function which defines the area of intersection of the laser beam and the full field of view of the telescope. The telescope's field of view is the ratio of aperture diameter to the focal length of the primary mirror. The light scattered within the full field of view can be collected by the primary mirror to contribute to the signal [5]. For a specified lidar system, the variability of $\xi(R)$ with the range R is governed by the aperture diameter. Here the optical fibre's numerical aperture and core diameter are analogous to the aperture stop which controls the field of view of the telescope. Based on Stelmaszczyk *et al.* [5] report on geometrical compression form-factor calculation, the overlap function variability for different aperture stop diameters is calculated for the lidar system at NARL as follows.

The laser light forms the illumination of a circle of the diameter of e at the focal plane of the primary mirror. It varies with R travelled in the atmosphere. It can be expressed as:

$$e(R)=f\left(\delta+\frac{g_0+T}{R}\right). \tag{3}$$

The change in position of the image is according to the change in the object's position because remote sensing objects are dynamic in nature. This displacement can be represented as:

$$\nu(R) = f\left(\frac{d_0 - \theta R}{R}\right), \tag{4}$$

where d_0 (300mm) is the distance between the telescope's axis to the laser location; δ is laser beam divergence; T is the primary mirror diameter; g_0 is the laser beam diameter at the beam exit; θ (0 mrad) is the inclination of a laser beam with respect to the telescope's axis; and s is the diameter of an aperture stop. An analytical function to describe Geometrical form factor (GCF) is given below. It is represented as $\xi(R)$:

$$\xi(R) = \begin{cases} 0 \\ \dfrac{\{\Psi_1(R) - \sin[\Psi_1(R)]\}s^2 + \{\Psi_2(R) - \sin[\Psi_2(R)]\}e^2(R)}{2\pi e^2(R)}, \\ 1 \end{cases} \tag{5}$$

where: a) $\xi(R)$=0, when $\nu(R) \geq s + e(R)/2,$ (6)

b) $\xi(R) = \dfrac{\{\Psi_1(R) - \sin[\Psi_1(R)]\}s^2 + \{\Psi_2(R) - \sin[\Psi_2(R)]\}e^2(R)}{2\pi e^2(R)},$

when it satisfies the condition $\dfrac{|s - e(R)|}{2} < \nu(R) < s + \dfrac{e(R)}{2}$ (7)

c) $\xi(R)$=1, when $\nu(R) < \dfrac{|s - e(R)|}{2}, e(R) \leq s,$ (8)

for: $$\Psi_1(R) = 2\arccos\left[\frac{s^2 + 4\nu^2(R) - e^2(R)}{4\nu(R)s}\right], \tag{9}$$

and $$\Psi_2(R) = 2\arccos\left[\frac{e^2(R) + 4\nu^2(R) - s^2}{4\nu(R)e(R)}\right]. \tag{10}$$

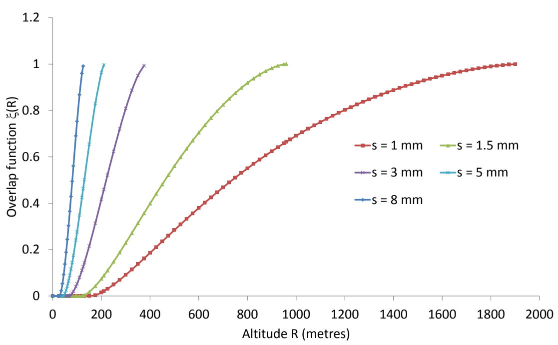

Fig. 1. Plot of the overlap function vs. altitude for different aperture diameters of the telescope.

It is apparent from Fig. 1 that the overlap function raises steeply with altitude for larger aperture stop diameters. The onset of overlapping of the laser beam with the telescope's field of view occurs at a lower altitude with an increasing stop diameter. Therefore larger stop diameters enable profiling of lower altitudes. For example, the overlap is zero up to an altitude of 200m for a stop diameter of 1mm whilst that for an 8mm stop diameter is 25m. The fibre specifications (numerical aperture NA and core diameter) govern the efficiency of image capture at the vicinity of the focal plane of the telescope and hence the SNR. As the fibre core diameter represents the stop diameter, fibre of a larger core diameter with low attenuation is preferable. However, large core fibres induce significant modal dispersion, bend losses and suffer from poor flexibility [6]. The commercial availability is also a limitation. Here we considered step index pure silica core fibre with fluorine doped cladding. The required numerical aperture of the fibre capable of accepting the back scattered light cone at the vicinity of the focal plane can be obtained as:

$$\frac{f}{T} = 0.5\left[\frac{1}{\mathrm{NA}^2} - 1\right]^{0.5}. \tag{11}$$

The NA turns out to be 0.148. The field of view of the current telescope by considering an effective aperture diameter of 300mm and focal length of 1000mm is 0.3rad. The range dependent image diameter produced by this telescope settles at ~0.5mm for altitudes ≥500m. Therefore a fibre of NA greater than 0.148 with a core diameter exceeding 0.5mm is preferable. The image blur in between the infinity focus and the near field focus attains a minimum value, the so called blur disk diameter, corresponds to the collection of all the backscattered light above certain altitude where the backscattering occurs within the full field of view of the telescope. This is termed as transitional altitude Z_t. The specified fibre faucet positioned at the location of a blur disk diameter corresponds to the maximum capture position. This location is unique for a specified fibre core diameter. The blur disk diameter d_b corresponding to different transitional altitudes can be obtained as:

$$d_b = \frac{f\delta + (T + g_0)f}{2z_t}. \tag{12}$$

The blur disk diameter corresponding to different transitional altitudes is shown in Fig. 2. It is readily apparent that larger blur disk diameters correspond to lower transitional altitudes and hence require large core fibre faucets for maximum light capture. We have considered low attenuation silica core fibre of numerical aperture and the core diameter equal to 0.39 and 1.5mm, respectively. This fibre can accept and guide the light of a full cone angle of 0.8 rad.

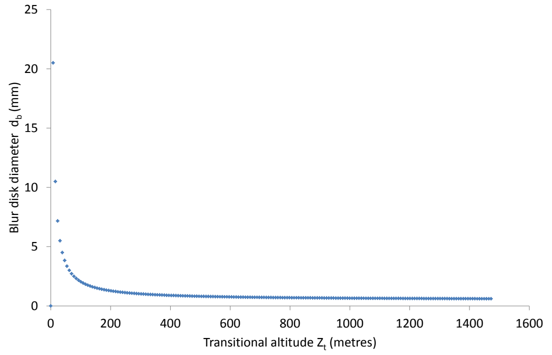

Fig. 2. Plot of a blur disk diameter and the corresponding transitional altitude.

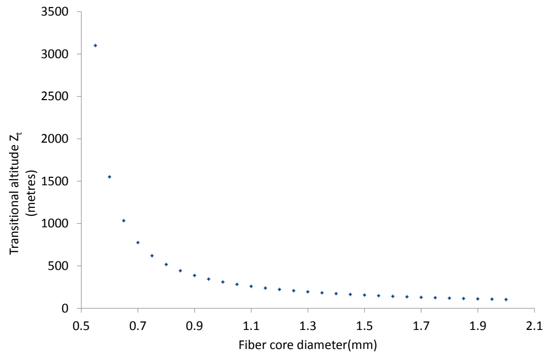

Fig. 3. Plot of a transitional altitude corresponding to the fibre core diameter (aperture).

The numerical aperture and the core diameter are 0.39 and 1.5 mm, respectively. The field of view of the current telescope by considering the effective aperture diameter of 300 mm and focal length of 1000 mm is 0.3 rad. The fibre can accept and guide a full cone of 0.8 rad angle. It is also required to position the fibre faucet at the maximum light capture position with respect to the infinity focus. From Figures 3 and 4, it is clear that the diameter of the fibre core imposes a limitation on the transitional altitude. In order to enable profiling of lower altitudes, we propose the use of a hot fused fibre bundle commercially available with Schott Glass, Germany [7]. Hot fused fibre bundles significantly lower light coupling losses because the interstitial spaces are drastically reduced via transformation of fibres to a hexagonal shape. This process increases the light capturing area by 20% as compared to conventional bundles. These bundles of high NA and bundle diameters up to 7.3mm could be a potential solution. By using a hot fused fibre bundle of diameter 7.3mm, the transitional altitude can be reduced to 22.7m. The attenuation of a fibre bundle is ~0.25dB/m whilst that for the 0.39 NA fibre is 0.02dB/m over a wavelength range of 550÷610nm [8] greater than that of 1.5mm core fibre over a wavelength range of 550÷610nm, which includes Raman back scattered wavelengths for oxygen (576nm) and nitrogen (607nm) using an excitation wavelength of 532nm. However, the larger aperture diameter may compensate for these losses and also facilitate profiling of lower altitudes. It is also important to keep the bundle length short to keep the losses to the minimum possible. This forms the subject of our current experimental investigations.

References

[1] A.M. Melesse *et al*., Sensors **51**, 3209 (2007).
[2] P. Wang *et al*., Phot. Lett Poland **2**, 6 (2010).
[3] J.R. Jenness *et al*., Appl. Optics **36**, 4278 (1997).
[4] J.V. Hey *et al*., Appl. Optics **50**, 5791 (2011).
[5] K. Stelmaszczyk *et al*., Appl. Optics **44**, 1323 (2005).
[6] A.A.P. Boechat *et al*., Appl. Optics **30**, 321 (1991).
[7] http://www.schott.com/china/chinese/download/284345_fo_light_it_right_e_without_tecspec.pdf
[8] https://www.thorlabs.com/thorproduct.cfm?partnumber=APCH1500

